Natural Hazards (2021) 107:1709–1729
https://doi.org/10.1007/s11069-021-04655-3

ORIGINAL PAPER

Research on displacement prediction of step-type landslide under the influence of various environmental factors based on intelligent WCA-ELM in the Three Gorges Reservoir area

Yong-gang Zhang[1] · Xin-quan Chen[2] · Rao-ping Liao[1] · Jun-li Wan[3] · Zheng-ying He[1] · Zi-xin Zhao[1] · Yan Zhang[4] · Zheng-yang Su[5]

Received: 23 September 2020 / Accepted: 19 February 2021 / Published online: 8 March 2021

Abstract
Landslides are one of the most destructive geological disasters and have been caused many casualties and economic losses every year in the world. The reservoir area formed by the world's largest hydropower project, Three Gorges Hydropower project of China, has become a natural testing ground for landslide prediction in the hope of reducing losses. In this paper, a new algorithm with strong optimization ability, the water cycle algorithm (WCA), is combined with the extreme learning machine (ELM) to improve the prediction accuracy of step-wise landslide. The gray relational grade analysis method was adopted to determine the main influencing factors of the landslide's periodic displacement. Then, the determined factors were used as the input items of the proposed WCA-ELM model, and the corresponding periodic displacement was used as the model output item. Taking the Liujiabao landslide in the Three Gorges Reservoir area as a case history, the proposed model was verified through a comparison with the measurements. The results showed that the model has a faster convergence rate and higher prediction accuracy than the traditional back-propagation neural network model and ELM-model. The water cycle algorithm is suitable for optimizing the accuracy of the extreme learning machine model in landslide prediction.

Keywords Step-type landslide · Displacement prediction · The Three Gorges Reservoir area · Intelligent water cycle algorithm · Extreme learning machine

✉ Rao-ping Liao
lrp_liao@tongji.edu.cn

[1] Key Laboratory of Geotechnical and Underground Engineering of Ministry of Education, and Department of Geotechnical Engineering, Tongji University, Shanghai 200092, China

[2] Xiamen Anneng Construction Co., Ltd., Xiamen 361000, China

[3] Railway Engineering Research Institute, China Academy of Railway Science Co., Ltd., Beijing 100081, China

[4] College of Civil and Transportation Engineering, Hohai University, Nanjing 210098, China

[5] Nanjing Hydraulic Research Institute, Nanjing 210029, China

1 Introduction

Landslide is one of the natural disasters in the world (Zhang et al. 2019a, b; Friele et al. 2020; Gao et al. 2020; Hu et al. 2020; Bar et al. 2020; Shaunik and Singh 2020; Obregon and Mitri 2019; Taoet al. 2020; Zha et al. 2017; Zhang et al. 2017), and it causes countless casualties and economic losses every year (Zhang et al. 2020b, c). It is well known that the bank slope of the reservoir is more prone to landslides due to the change of the original hydrogeological environment in the region caused by water storage in the reservoir area (Huang et al. 2020). The stable rock and soil mass on the bank slope of the reservoir are softened and consolidated again by rising the water level, also affected by periodic water-level fluctuation (Ma et al. 2018a; Yu et al. 2019), such as Baishuihe landslide and the Bazimen landslide in the TGRA (Delaney and Evans 2015). It may even lead to a series of multiple hazards such as barrier lake, dam breaks and floods (Fan et al. 2019; Wu et al. 2020; Zhang et al. 2020f; He et al. 2020a, b; Qiu et al. 2019; Qiu et al. 2020a, b; Zou et al. 2020; Mcquillan et al. 2020; Oggeri et al. 2019; Zhang et al. 2016; Mnzool et al. 2015; Basahel et al. 2019).

To minimize the losses caused by the landslides, an efficient and accurate early warning system is essential (Katsenis et al. 2020; Krkač et al. 2016; Yao et al. 2015). At present, researchers have mainly used physical models and data-driven models to predict the landslides (Huang et al. 2017; Zhang et al. 2020a). However, due to the large uncertainty in the physical properties of the landslide itself (Ma et al. 2018a, b) and the differences and uncertainties in the internal mechanism of the landslide (He et al. 2018; Xie et al. 2019), the physical model seems to be able to provide a reasonable theoretical explanation, but its application is actually limited. In addition, the landslide prediction test based on the physical model is very complicated and expensive (Thiebes et al. 2013; Zou et al. 2020). The data-driven model is based on powerful computing power and combined with machine learning methods, which makes it more efficient and easier to operate than physical models (Hegde and Rokseth 2020; Zhou et al. 2018).

In recent years, machine learning methods have been widely used to solve the engineering safety problems in various fields (Bao et al. 2019; Butcher et al. 2014; Hegde and Rokseth 2020; Zhang and Yang 2020; Temeng et al. 2020; Zakaria 2016; Wijesinghe and You 2016), and as one of the important methods of the data-driven model, it has been widely and successfully used in the landslide displacement prediction t (Guo et al. 2019; Luo et al. 2020). Generally, in the machine learning methods, the landslide displacement is decomposed into several components, including trend and periodic components (Du et al. 2012; Yang et al. 2019). The trend displacement presents a stable linear change. Therefore, most researchers use polynomial function to predict, and the results are relatively accurate. However, as the periodic displacement is caused by unstable factors, its fluctuation is large and the prediction is not accurate; thus, a more diversified prediction method is formed (Cao et al. 2015; Yang et al. 2019), such as BPNN (Du et al. 2012), artificial neural network (ANN) (Moayedi et al. 2019), recursive neural network (RNN) (Lian et al. 2015), long-short-term memory neural network (LSTM) (Yang et al. 2019), and least-squares support vector machine (LSSVM) (Lian et al. 2015). However, the BPNN model has the deficiency of slow convergence speed and easy to fall into the local minimum. The RNN does not capture long-term correlations in input sequences very well (Yang et al. 2019); the LSTM weights parameters slowly and time-consuming and so on. To make up for the shortcomings of the above methods, Lian et al. (2013) optimized the model of extreme learning machine (ELM) and achieved a good performance. In fact, the ELM algorithm

itself is famous for its nonlinear mapping ability and fault-tolerant ability, and it is also suitable for simulating the complex nonlinear relationship between the periodic displacement of landslide and influencing factors. The key is the optimization strategy of parameter weight.

The water cycle algorithm (WCA) based on the principle of natural water cycle is just such a new optimization algorithm, which has the characteristics of strong optimization ability, strong robustness and fast convergence speed. Therefore, WCA is adopted to replace the original calculation method of parameter weight of hidden layer in ELM to improve the prediction accuracy in this paper. The influencing factors of the input layer of the model were screened out by WCA-ELM model, and the prediction accuracy of the proposed WCA-ELM model is company of the gray relational grade (GRG) analysis (Yang et al. 2019) which were closely related to the periodic displacement of the landslide.

The corresponding periodic displacement of the influencing factors in the measured data of Liujiabao landslide from January to December 2013 was used as the learning dataset of the model input and output, after the prediction and accuracy analysis of the proposed WCA-ELM with that of the traditional BPNN and ELM models under the same dataset.

2 Introduction of ELM and WCA

2.1 ELM

The ELM was proposed by (Huang et al. 2006; Qiao et al. 2021; Zhang et al. 2021) on the basis of a single hidden layer feedforward neural network, including the input layer, hidden layer, and output layer, the structure of which can be seen in Fig. 1. External data are provided as an input to the network, and the hidden layer and output layer are composed of multiple neurons. Each layer is connected by a weight system, and the connection weights of the input layer and the hidden layer and the neuron deviation of the hidden layer are randomly set. For a detailed introduction to ELM, please refer to the following article (Huang et al. 2006, 2016; Lian et al. 2014; Tan et al. 2019; Zhang et al. 2020a).

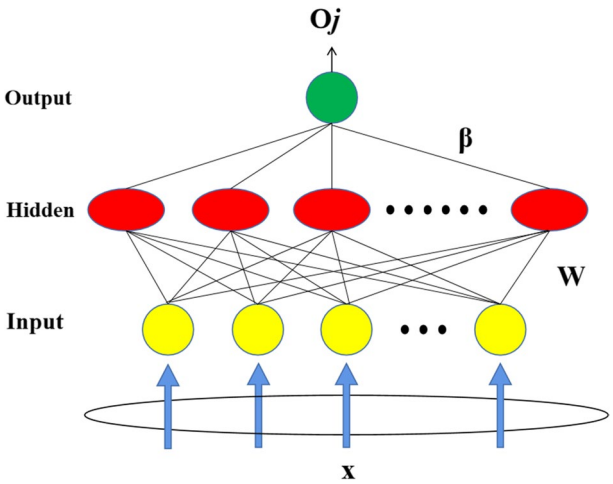

Fig. 1 The structure of ELM

The prediction process using the extreme learning machine algorithm includes the following steps: (1) determine the number of neurons in the hidden layer, the weight of the connection between the input layer and the hidden layer, and the offsets of neurons in the hidden layer; (2) calculate the output matrix H of the hidden layer by selecting an infinitely differentiable function as the activation function of the hidden layer neurons; (3) learn and get the weight matrix β of the output layer, and then the prediction is carried out (Tan et al. 2019).

2.2 WCA

The WCA is a new type of intelligence proposed by Hadi Eskandar et al. (Eskandar et al. 2012), which has been successfully used in the field of function optimization, mechanical, electric power, and civil engineering optimization because of its good random searchability, robustness, and optimization ability. It is inspired by the natural water cycle phenomenon in which water evaporates from the sea and forms rain, which forms streams, rivers, streams, and rivers flowing to the sea. Therefore, the specific process of the WCA is somewhat similar to the water cycle as follows (Eskandar et al. 2012; Sadollah et al. 2014; El-Fergany and Hasanien 2019), as Zhang introduced in Sect. 2 (Zhang et al. 2020d).

3 Proposed predictive model

3.1 Framework system

As shown in Fig. 2, a framework system for predicting the total accumulative displacement of the landslide was proposed, and formula 1′–11′ in the figure corresponds to 1–11 in Zhang et al. (2020d). This model uses most of the landslide observation data for big

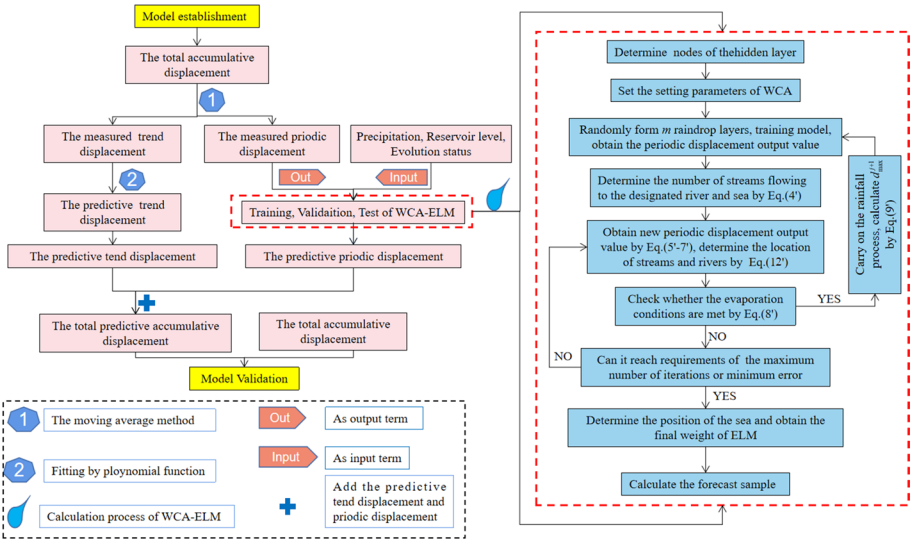

Fig. 2 The framework system for predicting the total accumulative displacement of the landslide

data matching and training. The training process includes trend term displacement, data processing, and periodic term WCA-ELM model. Finally, the remaining large amount of observation data is used for model verification. In the following sections, the creation process of the proposed predictive model is presented in detail.

4 Partition of the displacement time series

Displacement time series divides displacement into trend term and periodic term to establish the displacement prediction model (Du et al. 2012; Yang et al. 2019). The development of landslides is affected by many factors (Xu et al. 2018; Guo et al. 2019), which can be divided into two categories, trending factors and periodic factors. The trend term factors will cause the landslide displacement to increase monotonously with time. These factors include structural state, geological conditions, stress state, and so on. It is worth noting that the growth of the landslide displacement caused by the long-term creep, degradation, and weathering was not considered in this model. The periodic factors make the displacement of landslide change periodically with time, such as the change of water level and seasonal rainfall. Therefore, the cumulative displacement of the given time series in this article was equal to the sum of the two parts, which is expressed as follows:

$$S(t) = \mu(t) + \sigma(t) \tag{1}$$

where t denotes time; $S(t)$ denotes the accumulated displacement, $\mu(t)$ denotes the trend displacement, and $\sigma(t)$ denotes the periodic displacement.

5 Proposed model for landslide displacement prediction

The displacement of the trend items is constrained by many factors, showing a monotonous increase trend. Therefore, the polynomial function is very convenient and efficient to simulate the displacement growth curve of the trend term. In this paper, a polynomial function was selected to predict the displacement of the trend term by fitting the curve shape of the observed data. For detailed prediction methods, refer to chapter 4.3.

The influencing factors of the displacement of the period term include reservoir water level, rainfall, slope state. In this paper, through the combination of extensive ELM and WCA, the rainfall factor, reservoir water level change factor, and landslide evolution state factor selected by the gray relational grade (GRG) analysis method were used as the model input layer (Tan et al. 2017; Yang et al. 2019). The landslide periodic displacement was used as the model output layer. The network error was reversely calculated to solve the model weights, and WCA-ELM model was constructed. The WCA determines the ELM optimal connection weight realization steps:

(1) The model includes the input layer, hidden layer, and output layer. Rainfall factor, reservoir water level change factor, landslide evolution state factor as input; output landslide periodic displacement; the number of hidden layer nodes is determined according to empirical formula (Du et al. 2012).
(2) Set the control parameters of the water cycle algorithm: the total number of raindrop layers m; the number of rivers N_{river}; minimum $d_{\max}$; maximum number of iterations $k_{\max}$.

(3) m raindrop layers are randomly formed, and the position of each raindrop layer is $X_i = [x_{i,1}, x_{i,2}, \ldots, x_{i,N}]$ represents all the weights in the model. According to each group of weights and the forward calculation of ELM, the input samples of q group rainfall, reservoir water level change, and landslide evolution state are trained, and the periodic displacement output value of q group model is obtained, and then the cost function of each raindrop layer can be expressed as formula 12′,

where y_k is the actual osmotic pressure, $\hat{y}_k$ is the model calculated osmotic pressure, and q is the number of training samples.

(4) Choose the raindrop layer with the smallest cost function as the sea, and N_{river} smaller ones as the river. The number of streams flowing to the specified river and sea is determined according to formula (4′).

(5) In the confluence stage, the location of streams and rivers is changed according to formula (5′) ~ (7′). According to the new weights, train input samples of q group rainfall, reservoir water level changes, and landslide evolution status to obtain q group. The network output value is $\hat{y}_k$, and the cost functions corresponding to streams and rivers are calculated according to formula (12′). If the cost function of a stream is less than the cost function of a river, the position of the stream and the river is interchanged; if the cost function of the river is less than the cost function of the ocean, the position of the river and the ocean is interchanged.

(6) Formula 10′ is the criterion for determining whether to enter the evaporation stage. If it is not satisfied, then directly go to step (7′). If the conditions are met, it will enter the rainfall process, refer to 2.2.3 for the rainfall process, and finally calculate $d_{\max}^{j+1}$ by formula (9).

(7) When the maximum number of iterations or the minimum error is reached, the calculation ends; otherwise, return to step (5) to continue the calculation. The final sea position $X_{\text{sea}} = [x_1, x_2, \ldots, x_N]$ is the weight of the extreme learning machine.

(8) Based on the final weights, the model calculates the predicted samples to predict the periodic displacement of the landslide.

The model prediction effect was tested by the root-mean-square error (RMSE) and mean absolute percentage error (MAPE) (Eqs. 2 and 3) (Zhang et al. 2020e).

$$\text{RMSE} = \sqrt{\frac{1}{N}\sum_{i=1}^{N}\left(x_i - \hat{x}_i\right)^2} \tag{2}$$

$$\text{MAPE} = \frac{1}{N}\sum_{i=1}^{N}\left|x_i - \frac{\hat{x}_i}{x_i}\right| \tag{3}$$

where x_i represents the measured accumulative displacement of landslide; y_i represents the final predictive accumulative displacement of landslide; N represents the number of predicted values.

6 Application of the proposed method

6.1 Liujiabao landslide

The Liujiabao landslide is in Chongqing, China, on the right bank of the Yangtze River. The landslide has a longitude of 109°45′0″ and a latitude of 31°01′22″. The landslide has a nearly "tongue-shaped" shape. The front edge of the landslide directly reaches the Yangtze River. The trailing edge elevation of the landslide is 445 m, the leading edge elevation is 90 m, the relative elevation difference is 335 m, and the overall slope is 30°. The landslide is about 1000 m long from north to south, 60–1300 m wide from east to west, with an average thickness of 50 m, an area of about 930,000 m^2, and a volume of 46.55 million m^3 (Fig. 3a).

As shown in Fig. 3b, the profile of the landslide is "straight," with an average slope of about 35°, and the overall slope of the landslide is stepped. The material of the sliding body is mainly fragmentized mudstone and mudstone accumulation layer, the surface layer is mostly loose soil layer, and the foot of the steep slope is a mostly big rock. The volumetric ratio of soil to rock in the gravel soil is 6:4. The slip zone is the contact zone between the accumulation body and the bedrock, which contains silty clay and contains a small amount of gravel. The sliding bed is the argillaceous limestone with an occurrence of strike 330 330° and dip∠15°.

The Liujiabao landslide was ancient, and there had been many small landslides in history. The signs of landslide deformation had not been obvious since the 1990s. After the storage of the Three Gorges Reservoir reaches 135 m, the signs of deformation were not obvious. Professional monitoring results since 2007 indicate that the current deformation of the landslide body is in a state of constant creep deformation.

To avoid the occurrence of landslide disasters, since January 2007, nine GPS sensors were placed on the Liujiabao landslide to closely monitor its deformation process. The sensor position and elevation are shown in Fig. 3a, b.

Figure 4 contains the data of precipitation, reservoir water level, and GPS displacement between January 2007 and September 2013. The slope displacement shows a step characteristic with time. During the flood season between May and July of each year, the surface displacement suddenly increases and gradually stabilizes in the following time. The

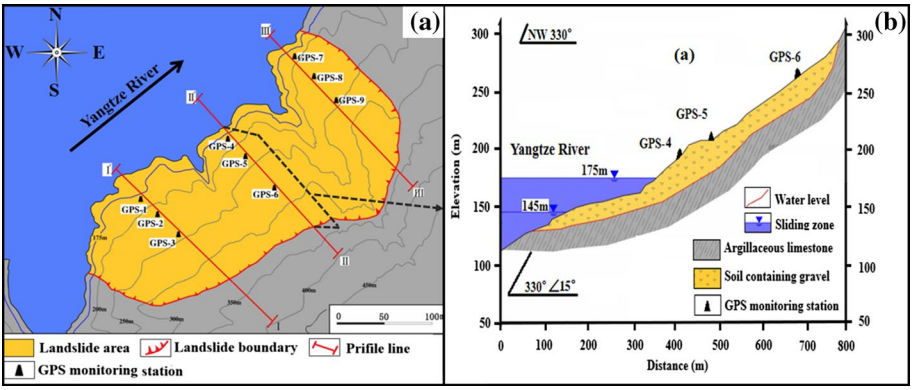

Fig. 3 The topographic map of landslide (a: plan of the landslide; b: sectional view of the landslide)

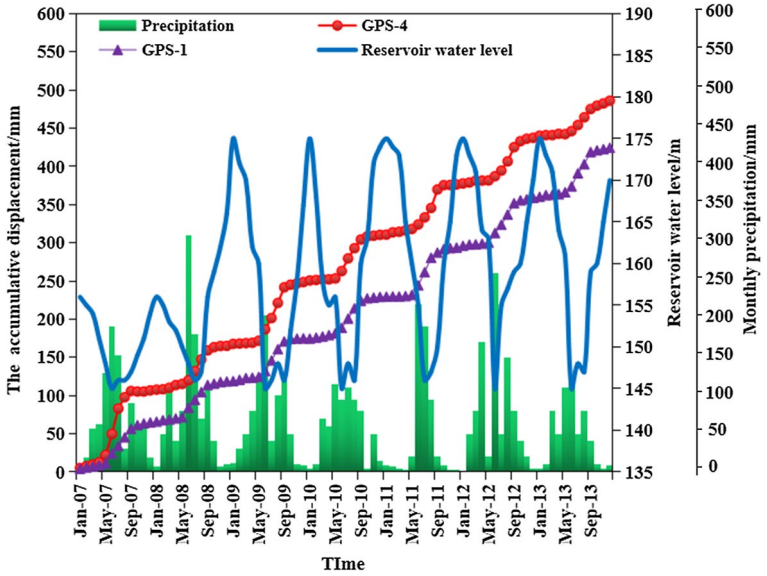

Fig. 4 Relationship of accumulative displacement, reservoir level, and precipitation with time in the Liujiabao landslide

deformation of the slope body near the river is more obvious, and relatively large vertical deformation was noticed at GPS-1, GPS-4, and GPS-7. Especially when the water level drops, the slope surface displacement increases significantly. When the water level rises or is relatively high, the displacement increases slowly.

7 Displacement decomposition

The observation points GPS-1 and GPS-4 obtained relatively large deformations in the study area, so the displacement data of these two observation points were selected to establish a prediction model. The displacement measurement data of GPS-1 and GPS-4 are decomposed into two parts of the period and trend (Fig. 5). During the establishment of the model, the observation data obtained from observation point GPS-1 and GPS-4 of the Liujiabao landslide during the period from January 2008 to December 2012 were selected as train dataset; and the data monitored from January 2013 to December 2013 were used for testing the predictive model (Fig. 6a).

Considering that the cumulative displacement contains trend and period terms, the moving average method can be used to extract the trend terms (Miao et al. 2017). The water level of the reservoir in the TGRA is between 145 and 175 m, so the moving average period was set at 12 months (Yang et al. 2019). The original displacement time formula is $S(t) = \{s_1, s_2, s_3, \ldots, s_t, \ldots, s_n\}$, and the displacement formula of the trend term is as follows:

$$\varphi(t) = \frac{s_t + s_{t-1} + \cdots s_{t-n+1}}{k}, (t = k, k+1, k+2, \cdots, n) \tag{4}$$

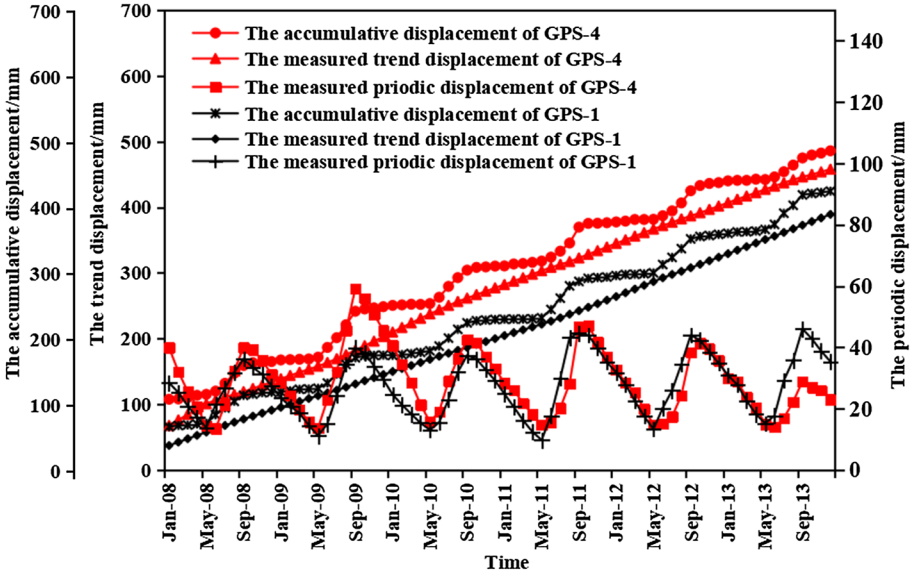

Fig. 5 Usage distribution of trend displacement and periodic displacement of GPS-1 and GPS-4 in the prediction process

where $\varphi(t)$ represents the displacement of the trend term at time t; S_t represents the accumulative displacement at time t; n represents the number of time notes monitored accumulative displacement; k represents the moving average cycle (set as 12).

The periodic term of the measured displacement $\sigma(t)$ is gained by subtracting the obtained trend term from the accumulative displacement.

$$\sigma(t) = S(t) - \mu(t) \tag{5}$$

where t denotes time; $S(t)$ denotes the accumulated displacement, $\mu(t)$ denotes the trend displacement, and $\sigma(t)$ denotes the periodic displacement.

8 Predictive method for trend term of displacement

Liujiabao landslide GPS-1 and GPS-4 observation points trend term displacement could be divided into two parts. Equation 6 was used for the least squares fitting and cubic polynomial fitting. The results of the fitting calculation are shown in Table 1. The comparison between the fitting results and the measured curve is shown in Fig. 6a.

$$\varphi(t) = at^3 + bt^2 + ct + d \tag{6}$$

where $\varphi(t)$ is the trend displacement at the time t and t is time; a, b, c, and d are the coefficients, where a cannot be zero.

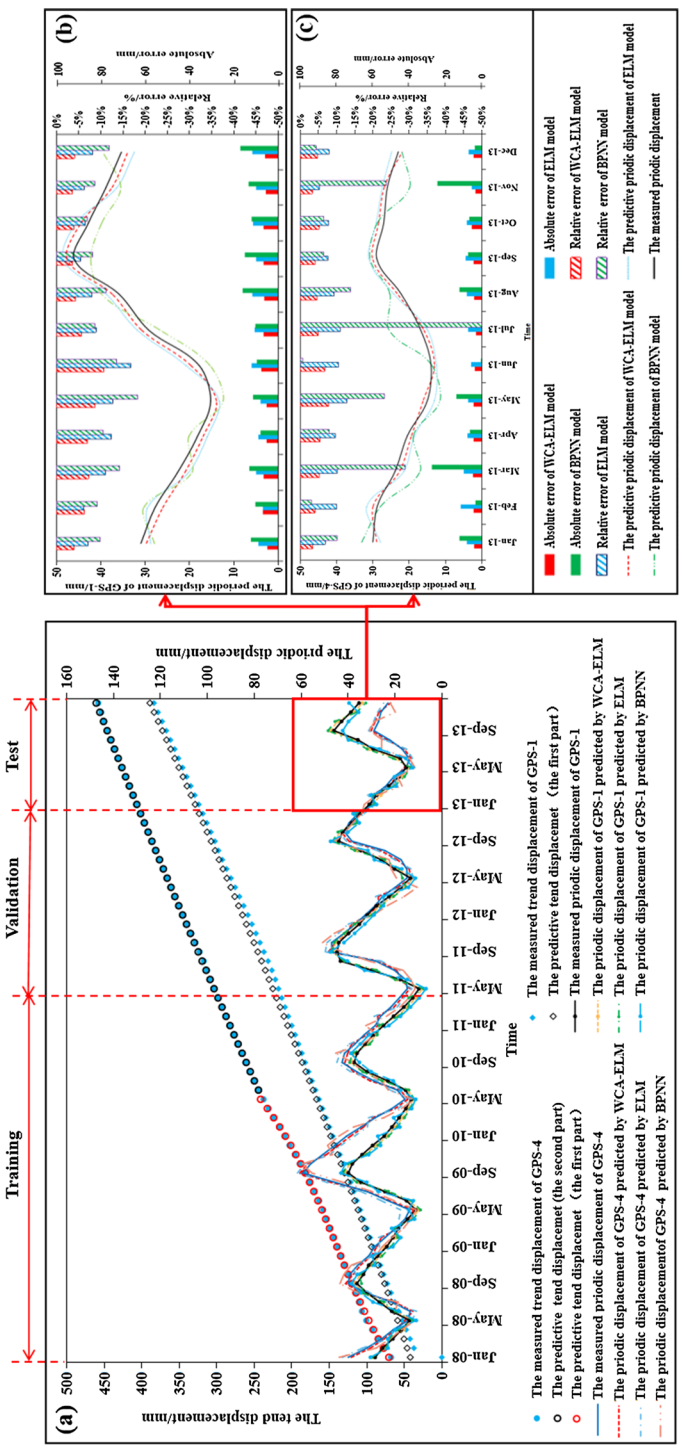

Fig. 6 Division of landslide displacement data and the predictive results of displacement of GPS-1 and GPS-4 (a: comparison of the predictive trend displacement and the measured of GPS-1 and GPS-4; b: comparison of BPNN, ELM, and WCA-ELM periodic displacement predictions of GPS-1; c: comparison of BPNN, ELM, and WCA-ELM periodic displacement predictions of GPS-4)

Table 1 Fitted results of trend displacement

Landslide	Monitoring points	Period	*a*	*b*	*c*	*d*	R^2
Liujiabao landslide	GPS-4	Jan 2008 to May 2010	0.0057	0.2243	7.8676	62.963	0.9983
		May 2010 to Jul 2013	– 0.0004	0.06	2.5905	126.14	0.9999
	GPS-1	Jan 2008 to Dec 2013	0.0002	0.0073	4.6666	34.759	0.9998

9 Periodic displacement prediction

9.1 Main controlling factors

In the WCA-ELM model, the triggers for the displacement of these periodic terms were used as the input sequence, and the output sequence was the periodic displacement. Periodic displacement was mainly affected by external trigger factors, so appropriate external trigger factors should be selected for model training.

Rainfall is one of the triggering factors of landslides, and its influence on landslide deformation has been extensively studied (Du et al. 2012; Xiong et al. 2019; Zhang et al. 2019; Koner and Chakravarty 2016). According to the actual monitoring results, it can be proved that the condition of Liujiabao landslide was affected by rainfall. During the rainy season, GPS-1 and GPS-4 experienced a significant increase in displacement (Fig. 7).

In addition to precipitation, periodic changes in the reservoir water level due to precipitation or human factors are a trigger for landslides in the reservoir area (Du et al.

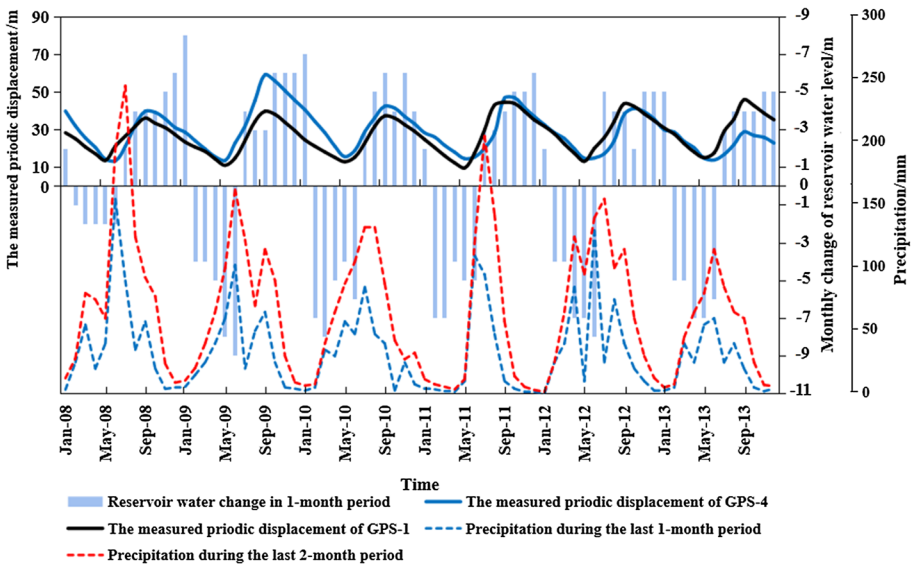

Fig. 7 Relationship between precipitation in late 1 and 2 months, reservoir water change in 1-month period, and the measured periodic displacement of GPS-1 and GPS-4

2012; Ma et al. 2018b; Yang et al. 2019). The drop in the reservoir water level will cause a greater rate of deformation of the landslide. It can be seen from the monitoring data that when the water level of the reservoir drops, the deformation rate of the landslide increases (Fig. 7).

In addition to the influence of external factors, the development of landslides will exhibit different characteristics at different times. In a stable situation, the landslide can remain stable even if it receives a large downward force. However, when the landslide is in an unstable stage, the weaker external force may lead to the instability of the landslide (Cao et al. 2015). Therefore, it was necessary to consider the current evolution of the landslide in the model. The input values of periodic displacement analysis are shown in Fig. 8.

GRG is used to analyze the correlation between periodic displacements and external triggering factors and landslide evolution status. When the value of GRG is greater than 0.8, it can be considered to have a high correlation (Lian et al. 2013). GRG value between the displacement of the periodic term and the input term in this model is shown in Fig. 8. It can be found that the GRG value is greater than 0.8, so the displacement of the input term and the periodic term has a strong correlation.

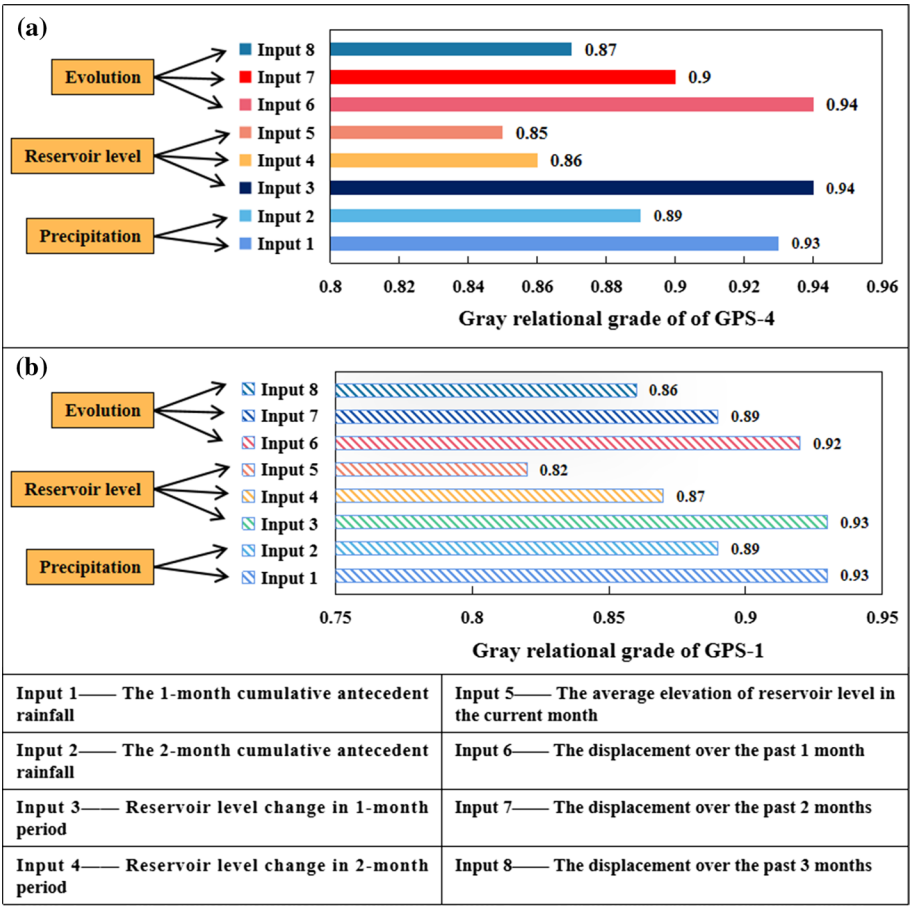

Input 1—— The 1-month cumulative antecedent rainfall	Input 5—— The average elevation of reservoir level in the current month
Input 2—— The 2-month cumulative antecedent rainfall	Input 6—— The displacement over the past 1 month
Input 3—— Reservoir level change in 1-month period	Input 7—— The displacement over the past 2 months
Input 4—— Reservoir level change in 2-month period	Input 8—— The displacement over the past 3 months

Fig. 8 The GRG of input items between inducing factors and periodic displacement

9.2 Model training

The data used to build the model were divided into two parts according to the role: data used for model training and data used for model verification. Determine the proportion of the two parts of data according to the quality and quantity of the two parts of data. For example, in this paper, the total number of raindrop layers in the model is $m = 60$, the number of rivers $N_{\text{river}} = 4$, the minimum value $d_{\max} = 0.001$, and the maximum number of iterations $k_{\max} = 1000$. Because the transfer function of the model is the Sigmoid function, the value range of this function is [0, 1], so the original data are normalized. The periodic displacement and key control factors of the landslide are normalized to [− 1, 1], 72 sets of training samples are put into the water circulation neural network model, and the training is carried out according to the model realization steps in Sect. 3, and the final weight of the model is obtained. The WCA-ELM model is implemented in Python through the Keras software package and uses TensorFlow as the backend. At the same time, the key control factors determined by GRG are input to the WCA-ELM model as an input sequence. During the WCA-ELM model training, the weight of the input sequence is not fixed. The WCA-ELM continuously updates the weights to determine the most appropriate input sequence weights.

The grid search method was used to obtain the appropriate WCA-ELM parameters. Various parameters were combined and used in the model during the search process. After all the combined calculations were completed, the model automatically feeds back the optimal parameter combinations. The length of the input sequence determined the number of historical data nodes. Therefore, it was very important to select the appropriate input sequence length through the grid search method, and the final length was 12. Figure 6a shows that the novel displacement prediction model can accurately predict the measured periodic displacement of the landslide.

For comparison, the ELM model and BPNN models were also applied to predict the periodic displacement of the Liujiabao landslide. Results verified the fine predictive ability of the used model.

9.3 The prediction of periodic term displacement

Figure 6b, c and Tables 2 and 3 show the comparison between the WCA-ELM, ELM, and BPNN model predicted periodic displacements and monitoring data at the GPS-1 and GPS-4 observation points of the Liujiabao landslide. For GPS-1, the RMSE and MAPE values of WCA-ELM were 1.54 mm and 5.71%, respectively, while the RMSE and MAPE of ELM were 2.5 mm and 9.13%, respectively, and at the same time the values of RMSE and MAPE of BPNN were 3.14 mm and 10.96%. The displacement predicted by WCA-ELM was more in line with the actual value than the displacement predicted by BPNN and ELM. The forecast curve of WCA-ELM was the same as the trend of the measurement curve, and the predicted value was very close to the true value. Especially in the peak area of September 2013, the prediction effect of WCA-ELM was significantly better than the BPNN model, the absolute error of WCA-ELM was 1.6 mm, and BPNN was 3.8 mm; during the period from February to March when the ELM model fluctuated greatly, the relative errors were 6.1% and 11.03%. WCA-ELM also showed satisfactory prediction results, with relative errors of 6.28% and 7.23%. And in the overall prediction period, WCA-ELM had the smallest absolute error and relative error among the three prediction models, the

Table 2 Accuracy of periodic displacement predicted using WCA-ELM, ELM, and BPNN models at position GPS-1

Time	The measured values (mm)	The WCA-ELM model			The ELM model			The BPNN model		
		Predictive values (mm)	Absolute error (mm)	Relative error (%)	Predictive values (mm)	Absolute error (mm)	Relative error (%)	Predictive values (mm)	Absolute error (mm)	Relative error (%)
13 Jan	31.0	29.7	1.2	3.97	28.7	2.2	7.14	27.9	3.1	9.92
13 Feb	27.8	26.0	1.7	6.28	29.5	1.7	6.10	30.3	2.6	9.19
13 Mar	22.6	21.0	1.6	7.23	20.1	2.5	11.03	19.4	3.2	14.29
13 Apr	18.2	17.0	1.3	6.96	16.0	2.3	12.35	20.1	1.9	10.57
13 May	15.2	13.9	1.3	8.65	13.3	1.9	12.69	12.4	2.8	18.35
13 Jun	17.8	19.7	1.9	10.61	20.8	3.0	16.83	15.4	2.4	13.59
13 Jul	29.2	30.8	1.6	5.56	31.8	2.6	8.92	26.7	2.6	8.74
13 Aug	35.8	37.3	1.5	4.28	38.7	2.9	8.05	39.8	4.0	11.14
13 Sep	46.0	47.7	1.6	3.53	48.5	2.5	5.40	42.3	3.8	8.21
13 Oct	42.8	44.5	1.7	3.88	45.6	2.8	6.47	39.8	3.0	7.02
13 Nov	38.8	37.5	1.4	3.53	36.4	2.5	6.37	35.5	3.3	8.59
13 Dec	35.3	33.9	1.4	4.06	32.4	2.9	8.23	39.6	4.2	11.93
Min	N/A	N/A	1.2	3.53	N/A	1.7	5.40	N/A	1.9	7.02
Max	N/A	N/A	1.9	10.61	N/A	3.0	16.83	N/A	4.2	18.35
Mean	N/A	N/A	1.5	5.71	N/A	2.5	9.13	N/A	3.1	10.96
RMSE	N/A	1.54	N/A	N/A	2.5	N/A	N/A	3.14	N/A	N/A

Table 3 Accuracy of periodic displacement predicted using WCA-ELM, ELM, and BPNN models at position GPS-4

Time	The measured values (mm)	The WCA-ELM model			The ELM model			The BPNN model		
		Predictive values (mm)	Absolute error (mm)	Relative error (%)	Predictive values (mm)	Absolute error (mm)	Relative error (%)	Predictive values (mm)	Absolute error (mm)	Relative error (%)
13 Jan	30.0	29.0	1.0	3.49	27.9	2.1	6.91	33.1	3.1	10.19
13 Feb	28.8	30.0	1.2	4.02	31.7	2.9	9.95	27.9	0.9	3.12
13 Mar	23.9	22.6	1.2	5.22	21.4	2.4	10.23	17.0	6.9	28.89
13 Apr	20.5	19.4	1.1	5.49	18.5	2.0	9.66	18.8	1.6	8.01
13 May	14.9	16.1	1.2	7.73	13.0	1.9	12.87	11.5	3.5	23.19
13 Jun	14.0	13.0	1.0	6.87	12.5	1.5	10.54	13.9	0.1	0.78
13 Jul	16.9	16.1	0.8	4.88	15.1	1.9	10.95	25.7	8.8	51.75
13 Aug	22.3	23.3	1.0	4.64	24.3	2.1	9.26	25.3	3.1	13.86
13 Sep	29.0	30.1	1.2	4.03	31.2	2.2	7.58	30.8	1.8	6.39
13 Oct	27.0	28.4	1.4	5.25	29.1	2.1	7.78	28.8	1.8	6.50
13 Nov	26.0	26.9	0.9	3.36	27.4	1.4	5.33	19.9	6.1	23.64
13 Dec	23.0	21.9	1.1	4.75	24.8	1.8	7.90	22.0	1.0	4.35
Min	N/A	N/A	0.8	3.36	N/A	1.4	5.33	N/A	0.1	0.78
Max	N/A	N/A	1.4	7.73	N/A	3.8	12.87	N/A	8.8	51.75
Mean	N/A	N/A	1.1	4.98	N/A	2.3	9.08	N/A	3.2	15.06
RMSE	N/A	1.10	N/A	N/A	2.05	N/A	N/A	4.12	N/A	N/A

maximum absolute error was 1.9 mm, the maximum relative error was 10.61%; BPNN had the largest absolute error and relative error. Besides, during the landslide warning period (May–July), the reservoir water level decreased and the displacement began to increase. At this time, the predicted value of WCA-ELM was more accurate than ELM and more accurately reflected the relationship between influencing factors and displacement.

The prediction accuracy of WCA-ELM is more obvious on GPS-4. The values of RMSE and MAPE for WCA-ELM of GPS-4 were 1.10 mm and 4.98%, respectively, while the values of RMSE and MAPE of ELM were 2.05 mm, respectively, and 9.08%; meanwhile, the RMSE and MAPE values of BPNN were 4.12 mm and 15.06%. The BPNN model had a large relative error in March, May, July, and November. The relative error exceeds 20% and reached a maximum value of 51.75% in November. At the same time, the entire prediction curve showed an obvious fluctuation. The predictive trend of the WCA-ELM model and the ELM model was the same, but the WCA-ELM had a better forecasting effect between February and July when the volatility of ELM was large. The forecasting trends of the WCA-ELM model and the ELM model were the same, but the relative errors of WCA-ELM from February to July were smaller than that of ELM, which means that WCA-ELM has better between February and July with greater fluctuations in ELM predictive effect. It is worth mentioning that, at the minimum (June) and maximum (September) displacements of the periodic term, although the absolute error of BPNN at June was only 0.1 mm, considering the large fluctuations in the surrounding time, this paper believes that the degree of dispersion was large, so the prediction result of WCA-ELM was closer to the actual measured value.

10 The prediction of the accumulative displacement

The cumulative displacement prediction results are shown in Fig. 9. The accumulative displacement is the sum of the trend term displacement and the period term displacement. Figure 9 illustrates the comparison between the predicted values of the WCA-ELM model of the observation points GPS-1 and GPS-4 and the accumulative displacement of in situ monitoring. This model has high prediction accuracy.

11 Discussion

Based on the above analyses, the WCA-ELM model has more accurate prediction capabilities and higher convergence speed than the ELM and the BPNN in the prediction of TGRA landslide displacement. In the WCA-ELM model, the weight of the ELM can be quickly analyzed based on GRG to find the optimal solution, which greatly improves the calculation speed.

The analyses of the Liujiabao landslide showed that the key factors affecting the displacement of the periodic term were rainfall and reservoir water level changes. It should be noted that as the triggering factors change, the learning rules during the training process would also change. The WCA-ELM model recorded and fully considered these changes during the learning process.

In terms of the landslide displacement prediction, the WCA-ELM model yielded better prediction than the BP model and ELM model. However, the neural network algorithms

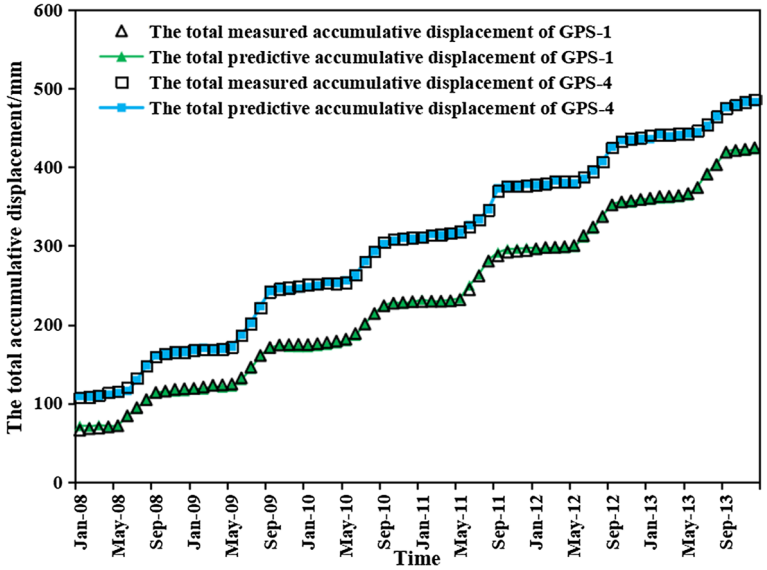

Fig. 9 Comparison of the total predictive accumulative displacement and the measured of GPS-1 and GPS-4

are based on a large amount of datum. It would be an interesting topic for increasing the prediction accuracy based on the limited datum in the future.

12 Conclusion

Many researchers have studied many neural network models to predict landslide displacement. In order to improve the calculation speed of neural network weights, this paper built a new prediction model based on the WCA-ELM model.

Liujiabao landslide displacement prediction in the TGRA, the WCA-ELM model has a speed advantage in solving weights. By constructing the relationship between the landslide conditions at different times and the learning rules recorded in the previous time of deformation evolution, the WCA-ELM model can effectively use historical information; at the same time, the WCA determines the optimal connection weight and deviation of ELM, which improves the prediction accuracy of the model.

In the prediction of gradual landslide displacement, this paper compares WCA-ELM with ELM and BP models. WCA-ELM has a smaller relative error and absolute error in the prediction and has more stable prediction results in the period where the other two models have larger errors. During the landslide warning period, WCA-ELM more accurately reflected the relationship between influencing factors and displacement.

In summary, the WCA-ELM model based on time series analysis can accurately predict the displacement of landslides and has the advantage of calculation speed and has the potential to establish a landslide warning system for TGRA.

Acknowledgement The authors appreciate the financial support provided by the Fundamental Research Funds for the Central Universities [No.2015XKMS035].

Author Contributions YZ helped in conceptualization and resources; XC contributed to data curation; LW and YZ helped in methodology; ZS helped in software; RL and ZY wrote—original draft; all authors have read and agreed to the published version of the manuscript.

Declaration

Conflicts of interest The authors declare no conflict of interest.

References

Bao Y, Han X, Chen J, Zhang W, Zhan J, Sun X, Chen M (2019) Numerical assessment of failure potential of a large mine waste dump in Panzhihua City. China Eng Geol 253:171–183. https://doi.org/10.1016/j.enggeo.2019.03.002

Bar N, Kostadinovski M, Tucker M (2020) Rapid and robust slope failure appraisal using aerial photogrammetry and 3D slope stability models. Int J Min Sci Technol 30:651–658

Basahel H, Mitri H (2019) Probabilistic assessment of rock slopes stability using the response surface approach—a case study. Int J Min Sci Technol 29(3):357–370

Butcher JB, Day CR, Austin JC, Haycock PW, Verstraeten D, Schrauwen B (2014) Defect detection in reinforced concrete using random neural architectures. Comput Aided Civ Infrastruct Eng 29:191–207. https://doi.org/10.1111/mice.12039

Cao Y, Yin K, Alexander DE, Zhou C (2015) Using an extreme learning machine to predict the displacement of step-like landslides in relation to controlling factors. Landslides 13:725–736. https://doi.org/10.1007/s10346-015-0596-z

Delaney KB, Evans SG (2015) The 2000 Yigong landslide (Tibetan Plateau), rockslide-dammed lake and outburst flood: review, remote sensing analysis, and process modelling. Geomorphology 246:377–393. https://doi.org/10.1016/j.geomorph.2015.06.020

Du J, Yin K, Lacasse S (2012) Displacement prediction in colluvial landslides Three Gorges Reservoir, China. Landslides 10:203–218. https://doi.org/10.1007/s10346-012-0326-8

El-Fergany AA, Hasanien HM (2019) Water cycle algorithm for optimal overcurrent relays coordination in electric power systems. Soft Comput 23:12761–12778. https://doi.org/10.1007/s00500-019-03826-6

Eskandar H, Sadollah A, Bahreininejad A, Hamdi M (2012) Water cycle algorithm—a novel metaheuristic optimization method for solving constrained engineering optimization problems. Comput Struct 110–111:151–166. https://doi.org/10.1016/j.compstruc.2012.07.010

Fan X et al (2019) Prediction of a multi-hazard chain by an integrated numerical simulation approach: the Baige landslide, Jinsha River, China. Landslides 17:147–164. https://doi.org/10.1007/s10346-019-01313-5

Friele P, Millard TH, Mitchell A, Allstadt KE, Menounos B, Geertsema M, Clague JJ (2020) Observations on the May 2019 Joffre Peak landslides, British Columbia. Landslides. https://doi.org/10.1007/s10346-019-01332-2

Gao Y, Li B, Gao H, Chen L, Wang Y (2020) Dynamic characteristics of high-elevation and long-runout landslides in the Emeishan basalt area: a case study of the Shuicheng "7.23" landslide in Guizhou China. Landslides. https://doi.org/10.1007/s10346-020-01377-8

Guo Z, Chen L, Gui L, Du J, Yin K, Do HM (2019) Landslide displacement prediction based on variational mode decomposition and WA-GWO-BP model. Landslides 17:567–583. https://doi.org/10.1007/s10346-019-01314-4

He C, Hu X, Tannant DD, Tan F, Zhang Y, Zhang H (2018) Response of a landslide to reservoir impoundment in model tests. Eng Geol 247:84–93. https://doi.org/10.1016/j.enggeo.2018.10.021

He MM, Zhang ZQ, Zheng J, Chen FF, Li N (2020a) A new perspective on the constant m(i) of the hoek-brown failure criterion and a new model for determining the residual strength of rock. Rock Mech Rock Eng 53(9):3953–3967

He MM, Li N, Zhu J, Chen YS (2020b) Advanced prediction for field strength parameters of rock using drilling operational data from impregnated diamond bit. J Petrol Sci Eng 187:106847

Hegde J, Rokseth B (2020) Applications of machine learning methods for engineering risk assessment—A review. Saf Sci. https://doi.org/10.1016/j.ssci.2019.09.015

Hu Y-x, Yu Z-y, Zhou J-w (2020) Numerical simulation of landslide-generated waves during the 11 October 2018 Baige landslide at the Jinsha River. Landslides. https://doi.org/10.1007/s10346-020-01382-x

Huang G-B, Zhu Q-Y, Siew C-K (2006) Extreme learning machine: theory and applications. Neurocomputing 70:489–501. https://doi.org/10.1016/j.neucom.2005.12.126

Huang F, Yin K, Zhang G, Gui L, Yang B, Liu L (2016) Landslide displacement prediction using discrete wavelet transform and extreme learning machine based on chaos theory. Environ Earth Sci 75:1376. https://doi.org/10.1007/s12665-016-6133-0

Huang F, Huang J, Jiang S, Zhou C (2017) Landslide displacement prediction based on multivariate chaotic model and extreme learning machine. Eng Geol 218:173–186. https://doi.org/10.1016/j.enggeo.2017.01.016

Huang X, Guo F, Deng M, Yi W, Huang H (2020) Understanding the deformation mechanism and threshold reservoir level of the floating weight-reducing landslide in the Three Gorges Reservoir Area, China. Landslides. https://doi.org/10.1007/s10346-020-01435-1

Katsenis LC, Stamatopoulos CA, Panoskaltsis VP, Di B (2020) Prediction of large seismic sliding movement of slopes using a 2-body non-linear dynamic model with a rotating stick-slip element. Soil Dyn Earthq Eng. https://doi.org/10.1016/j.soildyn.2019.105953

Koner R, Chakravarty D (2016) Numerical analysis of rainfall effects in external overburden dump. Int J Min Sci Technol 26(5):825–831

Krkač M, Špoljarić D, Bernat S, Arbanas SM (2016) Method for prediction of landslide movements based on random forests. Landslides 14:947–960. https://doi.org/10.1007/s10346-016-0761-z

Lian C, Zeng Z, Yao W, Tang H (2013) Ensemble of extreme learning machine for landslide displacement prediction based on time series analysis. Neural Comput Appl 24:99–107. https://doi.org/10.1007/s00521-013-1446-3

Lian C, Zeng Z, Yao W, Tang H (2014) Extreme learning machine for the displacement prediction of landslide under rainfall and reservoir level. Stoch Env Res Risk Assess 28:1957–1972. https://doi.org/10.1007/s00477-014-0875-6

Lian C, Zeng Z, Yao W, Tang H (2015) Multiple neural networks switched prediction for landslide displacement. Eng Geol 186:91–99. https://doi.org/10.1016/j.enggeo.2014.11.014

Luo Z, Luo Z, Qin Y, Wen L, Ma S, Dai Z (2020) Developing new tree expression programing and artificial bee colony technique for prediction and optimization of landslide movement. Eng Comput 36:1117–1134. https://doi.org/10.1007/s00366-019-00754-9

Ma G, Hu X, Yin Y, Luo G, Pan Y (2018a) Failure mechanisms and development of catastrophic rockslides triggered by precipitation and open-pit mining in Emei, Sichuan, China. Landslides 15:1401–1414. https://doi.org/10.1007/s10346-018-0981-5

Ma J, Tang H, Liu X, Wen T, Zhang J, Tan Q, Fan Z (2018b) Probabilistic forecasting of landslide displacement accounting for epistemic uncertainty: a case study in the Three Gorges Reservoir area China. Landslides 15:1145–1153. https://doi.org/10.1007/s10346-017-0941-5

Mcquillan A, Canbulat I, Oh J (2020) Methods applied in Australian industry to evaluate coal mine slope stability. Int J Min Sci Technol 30(2):151–155

Miao F, Wu Y, Xie Y, Li Y (2017) Prediction of landslide displacement with step-like behavior based on multialgorithm optimization and a support vector regression model. Landslides 15:475–488. https://doi.org/10.1007/s10346-017-0883-y

Mnzool M, Ling W, Wei ZA (2015) Slope stability analysis of Southern slope of Chengmenshan copper mine China. Int J Min Sci Technol 25(2):171–175

Moayedi H, Mehrabi M, Mosallanezhad M, Rashid ASA, Pradhan B (2019) Modification of landslide susceptibility mapping using optimized PSO-ANN technique. Eng Comput 35:967–984. https://doi.org/10.1007/s00366-018-0644-0

Obregon C, Mitri H (2019) Probabilistic approach for open pit bench slope stability analysis—a mine case study. Int J Min Sci Technol 29(4):629–640

Oggeri C, Taddeo F, Alberto G (2019) Overburden management in open pits: options and limits in large limestone quarries. Int J Min Sci Technol 29(02):70–81

Qiao S, Tan J, Zhang Y, Wan L, Zhang M, Tang J, He Q (2021) Settlement prediction of foundation pit excavation based on the GWO-ELM model considering different states of influence. Advin Civ Eng. https://doi.org/10.1155/2021/8896210

Qiu L, Song D, Li Z (2019) Research on AE and EMR response law of the driving face passing through the fault. Saf Sci 17:184–193

Qiu L, Song D, He X, Wang E, Li Z, Yin S, Wei M, Liu Y (2020a) Multifractal of electromagnetic waveform and spectrum about coal rock samples subjected to uniaxial compression. Fractals. https://doi.org/10.1142/S0218348X20500619

Qiu L, Liu Z, Wang E, He X, Feng J, Li B (2020b) Early-warning of rock burst in coal mine by low-frequency electromagnetic radiation. Eng Geol 279:105755

Sadollah A, Eskandar H, Bahreininejad A, Kim JH (2014) Water cycle algorithm for solving multi-objective optimization problems. Soft Comput 19:2587–2603. https://doi.org/10.1007/s00500-014-1424-4

Shaunik D, Singh M (2020) Bearing capacity of foundations on rock slopes intersected by non-persistent discontinuity. Int J Min Sci Technol. https://doi.org/10.1016/j.ijmst.2020.03.018

Tan F, Hu X, He C, Zhang Y, Zhang H, Zhou C, Wang Q (2017) Identifying the main control factors for different deformation stages of landslide. Geotech Geol Eng 36:469–482. https://doi.org/10.1007/s10706-017-0340-7

Tan M, Yin K, Guo Z, Zhang Y, Yang Y, Zhao H, Zhang Y (2019) Landslide displacement prediction based on CEEMDAN method and particle swarm optimized-extreme learning machine model. Geol Sci Technol Inf 38:165–175. https://doi.org/10.19509/j.cnki.dzkq.2019.0619 (**In Chinese**)

Tao Z, Shu Y, Yang X (2020) Physical model test study on shear strength characteristics of slope sliding surface in Nanfen open-pit mine. Int J Min Sci Technol. https://doi.org/10.1016/j.ijmst.2020.05.006

Temeng VA, Ziggah YY, Arthur CK (2020) A novel artificial intelligent model for predicting airover-pressure using brain inspired emotional neural network. Int J Min Sci Technol 30(5):683

Thiebes B, Bell R, Glade T, Jäger S, Mayer J, Anderson M, Holcombe L (2013) Integration of a limit-equilibrium model into a landslide early warning system. Landslides 11:859–875. https://doi.org/10.1007/s10346-013-0416-2

Wijesinghe DR, You G (2016) Optimization of the catch bench design using a genetic algorithm. Int J Min Sci Technol 26(06):1011–1016

Wu Y, Huang Z, Zhao K, Zeng W, Gu QX, Zhang R (2020) Unsteady seepage solutions for hydraulic fracturing around vertical wellbores in hydrocarbon reservoirs. Int J Hydrog Energy 45:9496–9503

Xie J et al (2019) A new prediction method for the occurrence of landslides based on the time history of tilting of the slope surface. Landslides 17:301–312. https://doi.org/10.1007/s10346-019-01283-8

Xiong X, Shi Z, Xiong Y, Peng M, Ma X, Zhang F (2019) Unsaturated slope stability around the Three Gorges Reservoir under various combinations of rainfall and water level fluctuation. Eng Geol. https://doi.org/10.1016/j.enggeo.2019.105231

Xu C, Sun Q, Yang X (2018) A study of the factors influencing the occurrence of landslides in the Wushan area. Environ Earth Sci. https://doi.org/10.1007/s12665-018-7584-2

Yang B, Yin K, Lacasse S, Liu Z (2019) Time series analysis and long short-term memory neural network to predict landslide displacement. Landslides 16:677–694. https://doi.org/10.1007/s10346-018-01127-x

Yao W, Zeng Z, Lian C, Tang H (2015) Training enhanced reservoir computing predictor for landslide displacement. Eng Geol 188:101–109. https://doi.org/10.1016/j.enggeo.2014.11.008

Yu S, Zhang J, Ren X (2019) Numerical analysis of the seepage characteristics of slopes with weak interlayers under different rainfall levels. Appl Ecol Environ Res 17:12465–12478

Zakaria J (2016) Development of slope mass rating system using K-means and fuzzy c-means clustering algorithms. Int J Min Sci Technol 26(06):959–966

Zha Z, Ma L, Li KM, Ding XH, Xiao SS (2017) Comparative study of mining methods for reserves beneath end slope in flat surface mines with ultra-thick coal seams. Int J Min Sci Technol 27(06):1065–1071

Zhang Y, Yang L (2020) A novel dynamic predictive method of water inrush from coal floor based on gated recurrent unit model. Nat Hazards. https://doi.org/10.1007/s11069-020-04388-9

Zhang YN, Tang JX, Li GD, Teng JY (2016) Influence of depth-thickness ratio of mining on the stability of a bedding slope with its sliding surface in concave deformation. Int J Min Sci Technol 26(6):1117–1123

Zhang T, Cai Q, Han L, Shu J, Zhou W (2017) 3D stability analysis method of concave slope based on the Bishop method. Int J Min Sci Technol 27(02):365–370

Zhang L, Xiao T, He J, Chen C (2019a) Erosion-based analysis of breaching of Baige landslide dams on the Jinsha River, China, in 2018. Landslides 16(10):1965–1979. https://doi.org/10.1007/s10346-019-01247-y

Zhang Y, Zhu S, Zhang W, Liu H (2019b) Analysis of deformation characteristics and stability mechanisms of typical landslide mass based on the field monitoring in the Three Gorges Reservoir, China. J Earth Syst Sci. https://doi.org/10.1007/s12040-018-1036-y

Zhang L, Chen X, Zhang Y, Wu F, Guo F (2020a) Application of GWO-ELM model to prediction of Caojiatuo landslide displacement in the Three Gorge Reservoir Area. Water 12:1860

Zhang Y, Zhang Z, Xue S, Wang R, Xiao M (2020b) Stability analysis of a typical landslide mass in the Three Gorges Reservoir under varying reservoir water levels. Environ Earth Sci. https://doi.org/10.1007/s12665-019-8779-x

Zhang Y, Zhu S, Tan J, Li L, Yin X (2020c) The influence of water level fluctuation on the stability of landslide in the Three Gorges Reservoir. Arab J Geosci. https://doi.org/10.1007/s12517-020-05828-3

Zhang Y, Tang J, Liao R, Zhang M, Zhang Y, Wang X, Su Z (2020d) Application of an enhanced BP neural network model with water cycle algorithm on landslide prediction. Stoch Env Res Risk Assess. https://doi.org/10.1007/s00477-020-01920-y

Zhang Y, Tang J, He Z, Tan J, Li C (2020e) A novel displacement prediction method using gated recurrent unit model with time series analysis in the Erdaohe landslide. Nat Hazards. https://doi.org/10.1007/s11069-020-04337-6

Zhang X, Wu Y, Zhai E, Ye P (2020f) Coupling analysis of the heat-water dynamics and frozen depth in a seasonally frozen zone. J Hydrol. https://doi.org/10.1016/j.jhydrol.2020.125603

Zhang Y, Qiu J, Zhang Y, Wei Y (2021) The adoption of ELM to the prediction of soil liquefaction based on CPT. Nat Hazards. https://doi.org/10.1007/s11069-021-04594-z

Zhou C, Yin K, Cao Y, Intrieri E, Ahmed B, Catani F (2018) Displacement prediction of step-like landslide by applying a novel kernel extreme learning machine method. Landslides 15:2211–2225. https://doi.org/10.1007/s10346-018-1022-0

Zou Z, Yan J, Tang H, Wang S, Xiong C, Hu X (2020a) A shear constitutive model for describing the full process of the deformation and failure of slip zone soil. Eng Geol. https://doi.org/10.1016/j.enggeo.2020.105766